Journal of Experimental and Applied Physics
Journal Homepage: jeap.ppj.unp.ac.id
Vol. 2, No. 4, December 2024.
ISSN (Print): 2988-0378 ISSN (Online): 2987-9256

Analysis of Fe_3O_4/Graphene Oxide Magnetic Properties Synthesized from Corn Cobs Waste as A Potential Material for Chemotherapy Agents

Abdul Aziz, Yenni Darvina*, Ratnawulan, Rahmat Hidayat

Department of Physics, Universitas Negeri Padang, Padang 25131, Indonesia

Article History
Received : Dec, 16th 2024
Revised : Dec, 27th 2024
Accepted : Dec, 30th 2024
Published : Dec, 30th 2024

DOI:
https://doi.org/10.24036/jeap.v2i4.85

Corresponding Author
*Author Name: Yenni Darvina
Email: ydarvina@fmipa.unp.ac.id

Abstract: Cancer is a medical condition caused by mutations in cellular DNA that damage tissue cell function. The high prevalence of cancer in Indonesia needs to be observed with preventive treatments, one of them by applying nanomedicine for targeted drug delivery at cancer sites. It's specifically will potential to increase the efficacy of treatment and reduce the side effects. Fe_3O_4/Graphene Oxide (GO) nanocomposite has been widely studied as an efficient nanocarrier drug delivery for chemotherapeutic agents. Therefore, it's necessary to research the effect of using Fe_3O_4/GO as an alternative material in chemotherapy agent development. Variations in the composition of Fe_3O_4 and GO used can determine the ability of magnetic properties. This study aims to analyze the magnetic properties of Fe_3O_4/GO nanocomposites from corn cob waste by using the modified hummer method. The results of the study were identified using Vibrating Sample Magnetometer with composition variations of 20%:80%, 30%:70% and 40%:60%. Based on the hysteresis curve it was shown an increase in magnetic properties along with the amount of Fe_3O_4 in the mixture of Fe_3O_4/GO nanocomposite, with Saturation Magnetization (Ms) values of 18,2 emu/gram (20%: 80%), 23,2 emu/gram (30%:70%), and 31,1 emu/gram (40%:60%); Remanent Magnetization (Mr) values of 6,82 emu/gram (20%:80%), 8,86 emu/gram (30%:70%), and 12,3 emu/gram (40%:60%) and Intrinsic Coercivity (Hc) values of 0,0421 T (20%:80%), 0,0399 T (30%:70%), and 0,0424 (40%:60%). Based on these characteristics, this sample classified as superparamagnetic material, it can be used as an alternative material of nanocarrier drug delivery for chemotherapeutic agents.

Keywords: Corncob; Fe_3O_4/GO nanocomposite; VSM; Narrow Hysteresis Curve; Superparamagnetic.

How to cite:
A. Aziz, Y. Darvina, Ratnawulan and R. Hidayat, 2024, Analysis of Fe_3O_4/Graphene Oxide Magnetic Properties Synthesized from Corn Cobs Waste as A Potential Material for Chemotherapy Agents, *Journal of Experimental and Applied Physics,* Vol.2, No.4, 90-106. Https://doi.org/10.24036/jeap.v2i4.85

1. Introduction

The pathological process of cancer starts with aberrant cellular alterations brought on by genetic alterations in cell DNA. This aberrant tissue development grows quickly, causing damage to tissue cell function and even invasion of all organs in the body [1]. Cancer is one of the biggest causes of death globally, claiming an estimated 9,6 million lives worldwide [2]. It was confirmed by cancer prevalence result in 2018 reaching 994.529, becoming the fifth highest number of cases in the world and the fourth highest number of cancer deaths with a prevalence of 830,180 deaths. Cancer cases in Asia ranked 23rd with the prevalence of cancer in Indonesia in 2019 reaching a level of 21.392 cases, with an average death rate of 13,9 per 100.000 people. The province with the highest prevalence in Indonesia for cancer is in the Special Region of Yogyakarta (DIY) at 4,86 per 100,000 population, followed by the province of Central Java at 2,1% [3].

The high prevalence of cancer in Indonesia needs to be observed with preventive treatment and early detection that has been undertaken by health care providers. Cancer cases that are found at an early stage and get treatment quickly and appropriately will provide healing and a longer life expectancy. Therefore, it is important to do a routine examination periodically as an effort to prevent and early detection of cancer is very important because cancer is one of the most deadly diseases [4]. Currently, lots of therapeutic treatments have been developed for cancer treatment, including conventional chemotherapy drugs (such as cyclophosphamide, methotrexate, doxorubicin, fluorouracil). Several problems have surfaced in the use of conventional chemotherapy, including inappropriate distribution, effects on normal tissues, and relatively quickly drug metabolism before reaching the tumor site. One of the methods developed in an attempt to overcome these problems is using nanomedicine to target drugs to cancer specifically. Early stage detection of cancer cells and targeting cancer cells with sufficient accuracy to improve toxicity selectivity are important topics in the research of chemotherapeutic agents for cancer treatment [5].

Chemotherapeutic agents are widely used in the treatment of cancer. The specialized delivery of chemotherapeutic agents to the cancer site has the potential to improve treatment effectiveness and reduce side effects. There are 3 main priorities to establish a drug delivery system using stabilized nanoparticles, namely (1) the system must have sufficient physicochemical stability so that the drug does not dissociate or decompose from the delivery system before reaching the site of the drug action, (2) after reaching the target of action, the delivery system must release the drug in sufficient quantities to cause a therapeutic effect, (3) the delivery system used (carrier) must be degradable and can be eliminated from the body to avoid long-term toxicity or immunogenicity [6].

Drug delivery using nanoparticles is useful for improving the effectiveness, efficiency of the applied drug, and increasing drug safety by preventing the drug from reacting in unexpected places [7]. Nanoparticles are colloidal particles that have a diameter of 1-10 nm, and are formulated using biodegradable polymers. The small size of nanoparticles can increase the solubility of active substances or drugs because the surface area increases so that it expands. This causes the distribution of the active substance to the target site through the bloodstream to be easier and the ability of absorption to the target site to be greater [8].

Based on the research conducted by Hanh [9] claimed that Fe_3O_4 and GO can be applied as nanocarrier drug delivery by utilizing the magnetic properties of Fe_3O_4 and the biocompatibility of GO. In utilizing superparamagnetic iron oxide (Fe_3O_4) nanoparticles in living organisms, the nanoparticles must be coated with biocompatible and biodegradable substances. Uncoated iron oxide (Fe_3O_4) nanoparticles have high surface activity and are easily aggregated, but after coating with GO, the nanoparticles are biocompatible and can be easily dispersed. In addition, the functional groups formed allow conjugation with other bioactive molecules or drugs [10]. The synthesis of GO with the right method is required to produce proper functional groups.

Corn cobs have a high content of carbon compounds, namely cellulose (41%) and hemicellulose (36%), which is high indicating that corn cobs have potential as an active charcoal production material. In addition, corn cobs also have a low ash content of 0,91%. Activated charcoal from this cob has several advantages including good potential as the carbon content is greater than the ash content, easy to make, the raw material is easily available and abundant, easy to use, safe, and durable [11]. Along with the development of science, corn cobs that have been processed into charcoal through the combustion process can be utilized as materials for the production of nanocomposite materials [12].

Nanocomposites are a type of material that combines two components, the matrix as reinforcement and the filler as a filling agent [13]. Fe_3O_4 is one type of nanoparticle known as magnetite. Fe_3O_4 has several advantages including good magnetic properties, low toxicity, and biocompatibility in physiological environments. Meanwhile, GO has advantages in the synthesis process, solubility, customizable conductivity, large surface area, biocompatibility, as well as being an abundant material source in nature and economically affordable [14]. Adding Fe_3O_4 to GO will provide the required magnetic properties to GO, so that these nanoparticles have superior properties including good biocompatibility, superparamagnetic properties, low production costs, and low environmental toxicity [15]. While both material have been the subject of intensive and separate research, there is still limited research on Fe_3O_4/GO nanocomposites.

Therefore, the analysis of the magnetic properties of Fe_3O_4/GO on Corn Cobs is expected to provide an alternative solution in producing eco-friendly and efficient nanocomposite materials and revealing the potential use of organic waste as a potential source of alternative raw materials. The purpose of this study is to identify the effect of composition variation on the characteristics of magnetic properties of Fe_3O_4/GO nanocomposites synthesized from corn cob waste base material using the modified hummer method.

2. Materials and Method

This research was experimental. It used a Vibrating Sample Magnetometer (VSM) to interpret magnetic results in the form of magnetic quantities as changes in the external magnetic field, represented by hysteresis curves, including Saturation Magnetization (Ms), Remanence Magnetization (Mr), and Intrinsic Coercivity (Hc). The analysis of characterization results using the Vibrating Sample Magnetometer (VSM) was processed with OriginPro 8.5.1 software to combine hysteresis curves for three variations of Fe_3O_4/GO nanocomposite compositions.

The materials used in this experiment included GO powder made from corn cob waste, sodium hydroxide (NaOH), sodium nitrate ($NaNO_3$), 98% sulfuric acid (H_2SO_4), potassium permanganate ($KMnO_4$), 30% hydrogen peroxide (H_2O_2), and distilled water. The tools used

were a mortar and pestle, a 100-mesh sieve, a measuring cup, an Erlenmeyer flask, a magnetic stirrer, an oven, a furnace, a vaporizer cup, a digital balance, a funnel, a volumetric flask, a baking pan, a volume pipette, centrifuge tubes, a centrifuge, a magnetic stirring rod, a fume hood, a spatula, a stirring rod, a distilled water spray bottle, and an ultrasonic device.

GO can be synthesized by oxidizing Graphite to Graphite Oxide which is then exfoliated to GO. The properties of this material are highly dependent on the synthesis method which affects the quantity and type of oxygen-containing groups in the formed GO. Unlike graphene, GO is hydrophilic, making it relatively easy to make water-based suspensions or organic solvents [16]. One method that is frequently used for synthesizing GO is the Hummer method. This method is a fairly quick conventional method used for the synthesis of GO. In this method, the reaction mixture consists of adding potassium permanganate, sulfuric acid, and a small amount of sodium nitrate. The reaction time ranges between 8 and 12 hours. This method is much safer as it avoids the formation of ClO_2 which is explosive. At the end of the reaction, the excess potassium permanganate is neutralized with an aqueous solution of H_2O_2. Unfortunately, this method is not eco-friendly due to the release of NOx during the reaction [17].

In this research, oxidation was performed using the modified Hummers method. GO was synthesized by oxidizing graphite, employing one of the principal methods by Brodie, Hummers, or Staudenmaier, which offered several advantages over established reduction techniques. First, the reaction was completed in a few hours. Second, $KClO_3$ was replaced with $KMnO_4$ to enhance safety by avoiding the formation of explosive ClO_3 . Third, the use of $NaNO_3$ instead of fuming HNO_3 prevented the production of acid mist. The modified Hummers method gained considerable interest due to its high efficiency and satisfactory safety during graphite oxidation. [18]. Pure graphite was the main raw material for the production of GO. However, pure graphite had a high cost. Consequently, researchers increasingly synthesized GO using naturally available graphene sources, such as activated carbon. Activated carbon, an organic material with high carbon content, was produced from various sources, including corn cobs.

The research was conducted through several stages of synthesis and characterization as follows:

1. Sample Preparation

Sample preparation was carried out by cleaning the corn cob waste, cutting it into small pieces, and drying it under the sun for 3 days. The water content of the corn cobs was then evaporated using an oven at 100°C for 1 hour [19]. After that, the corn cobs were heated in a furnace at 400°C for 2 hours until they transformed into biochar. The biochar was then pulverized using a mortar and pestle to form charcoal powder, which was subsequently filtered through a 100-mesh sieve.

2. Carbon Activation Stages

The activation stage of corn cob charcoal was performed after the corn cob was pulverized into powder. The initial activation stage began by preparing a NaOH solution using 100 mL of distilled water, measured with a measuring flask, and mixed with 8 grams of solid NaOH. The solid NaOH was then completely dissolved in distilled water, forming a homogeneous solution. Next, 8 grams of corn cob charcoal powder were placed into 250 mL beakers, and 100 mL of NaOH solution was poured into each, ensuring that the charcoal was submerged in the solvent.

The soaking procedure lasted for 24 hours, after which sediment formed at the bottom of the beaker. The next step involved straining the sediment using filter paper and a funnel to separate the liquid from the corn cob charcoal powder. The filter paper, moistened with distilled water, was placed in the funnel to filter the mixture of corn cob charcoal powder and NaOH solution. The filtered corn cob charcoal powder was then transferred into a vaporizer cup. The activated corn cob charcoal powder was dried for 3 hours at 105°C in an oven [20].

3. GO Preparation

GO was synthesized using the modified Hummers method. The synthesis began by mixing 1.5 grams of activated carbon powder from corn cob and 0.75 grams of $NaNO_3$ into a 250 mL Erlenmeyer flask. Then, 34,5 mL of 98% H_2SO_4 was added to the mixture [21]. The mixture was stirred for 2 hours and 20 minutes in an ice bath, maintaining temperatures between 0 and 5°C at a constant speed of 250 rpm. After that, the ice bath was removed, and 4.5 grams of $KMnO_4$ was added slowly without the ice bath for 30 minutes at about 35°C. After 30 minutes, 69 mL of distilled water was carefully added using a dropper while stirring for 20 minutes. The temperature increased upon adding the distilled water due to the endothermic reaction, and it was essential to keep the temperature below 50°C to observe the oxidation process, which was marked by a dark brown color change and the appearance of bubbles. Then, another 100 mL of distilled water and 1.5 mL of 30% H_2O_2 were added. The addition of H_2O_2 aimed to remove any remaining $KMnO_4$ or stop the reaction, causing the solution to turn yellow, indicating the presence of Graphite Oxide. Finally, 50 mL of distilled water was added, and graphite oxide was formed [22].

4. Sonication and Neutralization of GO

Sonication and neutralization of graphite oxide were conducted once the solution turned yellow, indicating the formation of graphite oxide. The graphite oxide mixture was sonicated for 2 hours to exfoliate the graphite into graphene [23]. Next, the solution was left to sediment for 1 day, allowing the liquid and solid phases to separate [24]. After that, the centrifugation process was carried out using a microcentrifuge at 4000 rpm for 15 minutes to separate the solid and liquid phases. The centrifugation procedure was followed by manual neutralization of GO, where the GO powder was precipitated, and distilled water was replaced repeatedly until the pH reached neutral (7). Once the neutral pH was achieved, the GO was oven-dried at 105°C for 1 hour [25].

5. Characterization of GO

After the GO was formed, the samples were characterized using XRD and FTIR procedures to analyze the obtained GO.

6. Synthesis of Nanocomposite Fe_3O_4/GO

The synthesis of Fe_3O_4/GO nanocomposites started by mixing the Fe_3O_4/GO with various composition ratios (20%:80%, 30%:70%, and 40%:60%). The mixing process was carried out using the ball milling method at a speed of 3000 rpm for 180 seconds [26]. The purpose of this step was not only to mix the materials but also to achieve homogenization of the particle size.

7. Stage of Nanocomposite Characterization of Fe_3O_4/GO

The Fe_3O_4/GO nanocomposites from corn cob were characterized using analytical methods, such as X-Ray Diffraction (XRD) to analyze the crystal size and structure, Fourier Transform Infrared (FTIR) spectroscopy to examine the functional groups, and Vibrating Sample Magnetometer (VSM) to assess the magnetic properties of the sample.

3. Results and Discussion

The XRD characterization was performed to confirm the effectiveness of the carbon activation process, the diffraction patterns displayed in Figure 1 as follows:

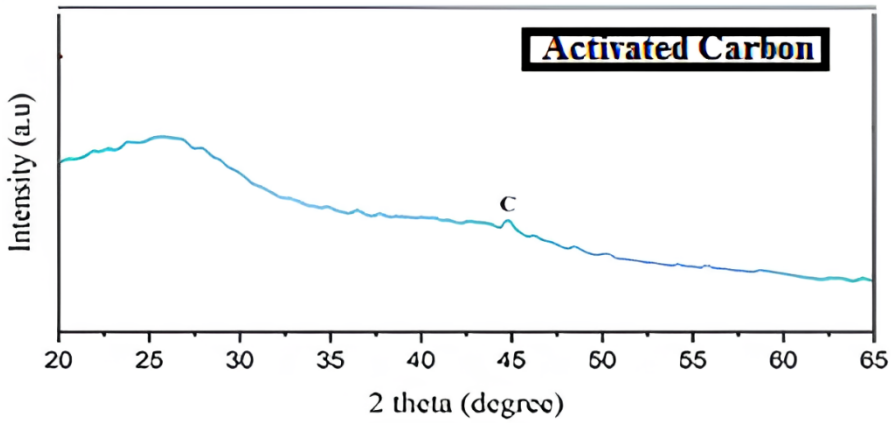

Figure 1. The results of XRD Characterization Activated Carbon from Corn Cob

The XRD characterization results shown in Figure 1 depict the diffraction pattern of the activated carbon. The XRD pattern was obtained using CuKα radiation (λ = 1,541 Å) over a 2θ range of 20° to 65°. Analyzing the diffraction pattern reveals that carbon activation occurred in the corn cob charcoal powder, as indicated by the C diffraction peak observed at a 2θ angle of 44,6° corresponding to the (111) plane.

The interpretation results of the XRD analysis for the samples are presented in Table 1 and Table 2 below:

Table 1. Significant peak on Activated Carbon

No	Pos.[º2Θ]	d-spacing[Å]	Ir[%]	FWHM Left [º2Θ]	Atom
1	44,58604	2,03061	100	0,3744	C

Table 2. Crystallite size calculation from the XRD for Activated Carbon

Pos.[º2Θ]	FWHM	D=(0,9 λ)/(β CosΘ)/2))	Average
44,58604	0,3744	22,93281218	22,93281218

Table 1 shows the diffraction pattern of activated carbon, indicated by the presence of a C peak in the XRD pattern at a 2θ angle of 44,5°, corresponding to the diffraction hkl (111) plane. This peak aligns with the JCPDS (Joint Committee Powder Diffraction Standard) result No. 80-0017 Determination of suitability crystal structure formed is done by matching each peak that appears on the diffractogram at angle values 2θ and d the results of the analysis with data from JCPDS (Joint Committee Powder Diffraction Standard) so that obtained information on the orientation of the of the crystals formed. If all crystal plane orientations are identified it is

confirmed that the crystal structure has conformity. Table 2 presents the analysis of the diffraction pattern, the sample has a cubic structure indicated by the Miller index (111) with an activated carbon crystallite size of 22,93 nm. Where D is the crystallite size, λ is the wavelength of CuKα (1,5405 Å), β is the full width half maximum (FWHM) (hkl), and θ is the Bragg angle.

The XRD characterization was performed to analyze the GO obtained. Diffraction patterns were obtained as shown in Figure 2 as follows:

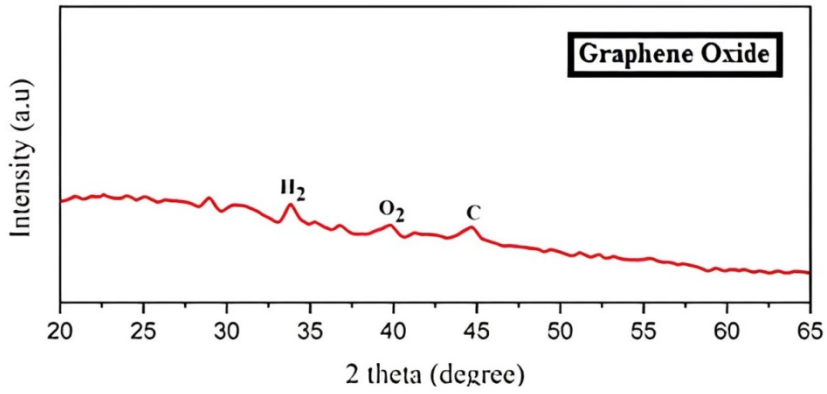

Figure 2. The results of XRD Characterization on GO

The XRD characterization results in Figure 2 display the diffraction pattern of GO. These patterns were obtained using CuKα radiation (λ = 1,541 Å) over a 2θ range of 20° to 65°. The diffraction pattern of GO is identified by the presence of C, O_2, and H_2 peaks.

The interpretation results of the XRD analysis for the samples are presented in Table 3 and Table 4 below:

Table 3. The results of Each Significant Peak on GO

No	Pos.[°2Θ]	d-spacing[Å]	Ir[%]	FWHM Left [°2Θ]	Atom
1	33,65834	2,66282	31,4	0,51168	H_2
2	39,58498	2,27674	100	0,818688	O_2
3	44,4094	2,03997	61,4	0,614016	C

Table 4. Crystallite Size Calculation From XRD For GO

Pos.[°2Θ]	FWHM	D=(0,9 λ)/(β CosΘ)/2))	Average
33,65834	0,51168	16,22058473	
39,58498	0,818688	10,31291715	13,5027029
44,4094	0,614016	13,97460692	

Table 3 shows that the diffraction pattern of GO is identified by the presence of C, O_2, and H_2 peaks in the XRD pattern at 2θ angles of 44,3° for the diffraction hkl (002) plane; 39,5° for the diffraction hkl (111) plane; and 33,6° for the diffraction hkl (101) plane. These peaks correspond to JCPDS (Joint Committee Powder Diffraction Standard) entries No. 80-0017, No.

85-1105, and No. 85-1256 . Where D is the crystallite size, λ is the wavelength of CuKα (1,5405 Å), β is the full width half maximum (FWHM) (hkl), and θ is the Bragg angle. The difference in FWHM values indicates peak broadening or widening of the curve at the diffraction peak. The larger FWHM changes and the decrease in intensity indicate the smaller the powder crystal size.. Meanwhile, Table 4 indicates the sample was hexagonal structure according by the miller index and the size of the GO crystallite was 13.5 nm.

The X-Ray Diffraction (XRD) characterization results for Fe_3O_4/GO nanocomposites with compositions of 40%:60%, 30%:70%, and 20%:80% were displayed in Figure 3 as follows:

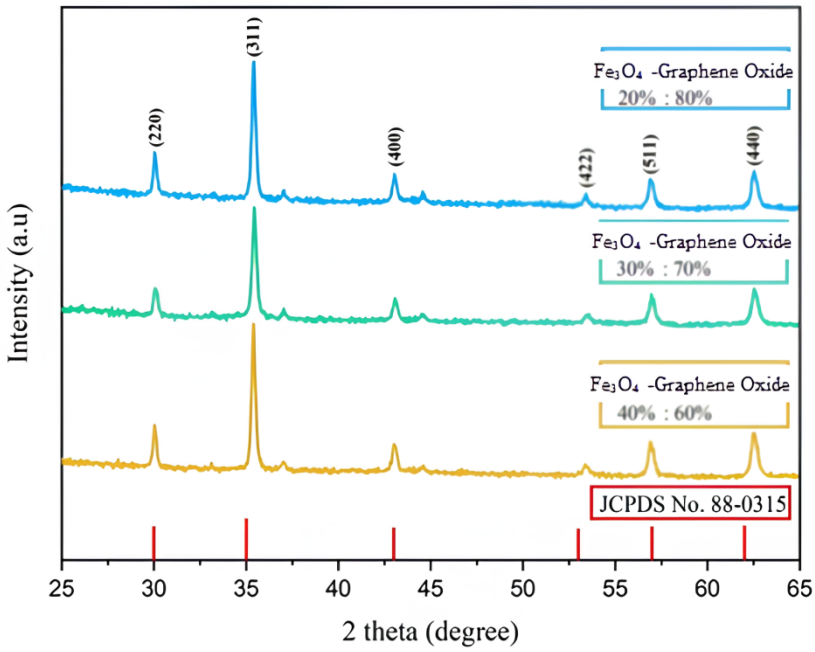

Figure 3. The XRD Result of JCPDS (Joint Committee Powder Diffraction Standard) No. 88-0315, and Variation of nanocomposite composition Fe_3O_4/GO

Based on Figure 3, the diffraction pattern of Fe_3O_4/GO nanocomposite with 3 variations of composition compared with JCPDS(Joint Committee Powder Diffraction Standard) No. 88-0315 by [27] as a standardization of the XRD results of Fe_3O_4/GO, which is at the peak of the 2θ = 30, 35, 43, 53, 57, dan 62 . Based on the peaks formed, it is in accordance with the standard XRD result for Fe_3O_4/GO (JCPDS (Joint Committee Powder Diffraction Standard) No. 88-0315). The miller index of each peak formed was diffraction hkl (220), (311), (400), (422), (511), and (440).

Table 5. Average results of the crystallite size of Fe_3O_4/GO nanocomposites composition of 40%: 60% ; 30% : 70%; and 20%: 80%

No	Composition Fe_3O_4/GO	Crystallite size
1	40% : 60%	42,93 nm
2	30% : 70%	39,19 nm
3	20% : 80%	45,32 nm

The results of the diffractogram pattern analysis used the Scherrer equation to determine the crystallite size. Based on Table 5, the average crystallite size of Fe_3O_4/GO nanocomposite witth composition 40% : 60% ; 30% : 70% ; and 20% : 80% in a row 42,93 nm, 39,19 nm and 45,32 nm.

The characterization results using FTIR was performed to analyze the GO obtained. infrared The spectrum were obtained as shown in Figure 4 as follows:

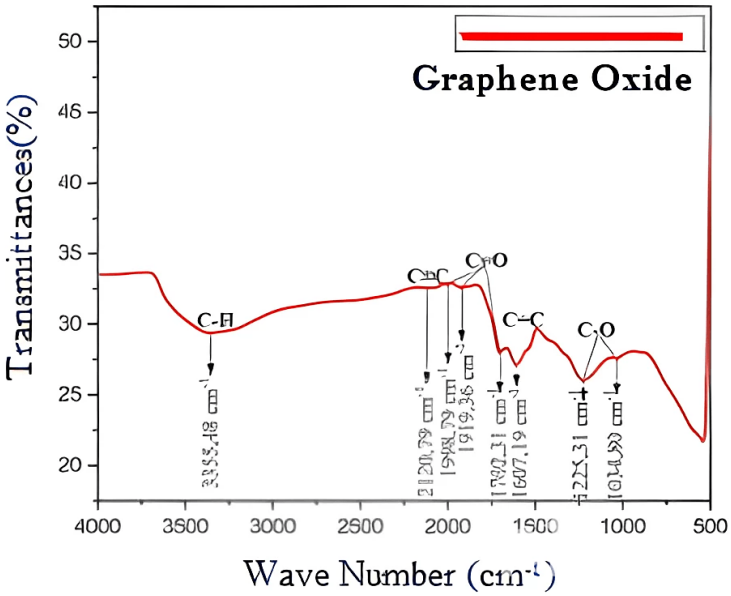

Figure 4. Results of FTIR Characterization on GO nanocomposites

Figure 4 shows the infrared spectrum from the FTIR characterization results, highlighting the relationship between intensity (% transmittance) and the energy range in wave numbers (cm^{-1}). A total of eight wave numbers were identified, as detailed in Table 6.

Table 6. Result of Absorption Peaks on GO nanocomposite composition

Peak To	Wave Number (cm^{-1})	Intensity (%Transmittances)
1	3355,48	29,39
2	2120,79	32,54
3	1998,79	32,76
4	1919,36	32,60
5	1702,31	27,98
6	1607,19	27,14
7	1225,31	26,07
8	1034,80	27,54

According to the data in Table 6, the formation of GO was attributed to the presence of C-O, C≡O, C=O, and O-H bonds [28]. From Figure 2 and Table 5, C-O wave peaks were

identified at wave numbers 1034.80 cm^{-1} and 1225.31 cm^{-1}; C=O wave peaks were observed at 1702.31 cm^{-1}, 1919.36 cm^{-1}, and 1998.79 cm^{-1}; a C≡O wave peak was detected at 2120.79 cm^{-1}; and an O-H wave peak was found at 3355.48 cm^{-1}.

The FTIR characterization results for Fe_3O_4/GO nanocomposites with compositions of 40%:60%, 30%:70%, and 20%:80% are presented in Figure 5.

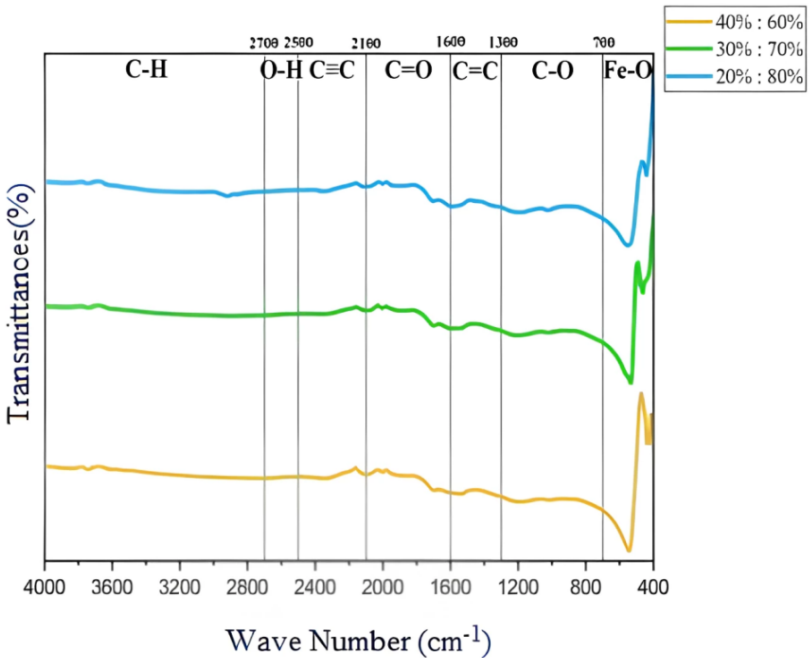

Figure 5. The composition variation FTIR spectra of Fe_3O_4 : GO nanocomposites, 40%:60%, 30%:70%, and 20%:80%.

Figure 5 displays the FTIR spectrum of Fe_3O_4 /GO nanocomposites with three composition variations: 40%:60%, 30%:70%, and 20%:80%. The data were processed using Origin software.

The FTIR characterization of the Fe_3O_4 /GO nanocomposite with a 40%:60% composition variation revealed several bond formations. A C-H bond was identified at wave numbers 3852.51 cm^{-1} and 3744.27 cm^{-1}, while an O-H bond appeared at 2714.98 cm^{-1}. The C≡C bond was observed at 2328.23 cm^{-1}, and the C=O bond was detected at wave numbers 2091.24 cm^{-1}, 2001.30 cm^{-1}, and 1698.52 cm^{-1}. Additionally, C=C bonds were noted at 1698.52 cm^{-1} and 1540.64 cm^{-1}, and C-O bonds at 1190.47 cm^{-1} and 1017.54 cm^{-1}. Lastly, Fe-O bonds were identified at wave numbers 543.26 cm^{-1}, 436.90 cm^{-1}, and 431.29 cm^{-1}.

The FTIR characterization of the Fe_3O_4 /GO nanocomposite with a 30%:70% composition variation identified several bond formations. C-H bonds were observed at wave numbers 3899.97 cm^{-1}, 3743.56 cm^{-1}, and 2906.49 cm^{-1}. C=O bonds appeared at 2085.68 cm^{-1}, 2002.62 cm^{-1}, 1902.21 cm^{-1}, and 1698.85 cm^{-1}. C=C bonds were detected at wave numbers 1584.59 cm^{-1} and 1540.96 cm^{-1}, while C-O bonds were present at 1203.75 cm^{-1} and 1023.32 cm^{-1}. Finally, Fe-O bonds were identified at wave numbers 534.65 cm^{-1} and 462.37 cm^{-1}.

The FTIR characterization of the Fe_3O_4 /GO nanocomposite with a 20%:80% composition variation revealed several bond formations. C-H bonds were observed at wave numbers 3899.60

cm^{-1}, 3744.33 cm^{-1}, and 2918.80 cm^{-1}. An O-H bond appeared at 2352.99 cm^{-1}, while C=O bonds were detected at 2089.42 cm^{-1}, 2000.83 cm^{-1}, 1902.09 cm^{-1}, and 1699.98 cm^{-1}. C=C bonds were identified at 1586.09 cm^{-1}, C-O bonds at 1178.61 cm^{-1} and 1022.28 cm^{-1}, and Fe-O bonds at 551.36 cm^{-1}, 466.28 cm^{-1}, and 439.30 cm^{-1}.

The FTIR analysis of Fe_3O_4/GO nanocomposites revealed the presence of C-H, O-H, C≡C, C=O, C=C, C-O, and Fe-O bonds. The Fe-O absorption peak was detected in the range of 400-700 cm^{-1}. According to research [29], the detection of Fe-O absorption peaks indicates that Fe_3O_4 has been successfully composited with GO. The vibrations of GO in the Fe_3O_4/GO composite were observed at absorption peaks around 1100-1300 cm^{-1} and 1400-1600 cm^{-1} [30].

The analysis of the magnetic properties of Fe_3O_4/GO nanocomposites synthesized from corn cob waste provided values for Saturation Magnetization (Ms), Remanent Magnetization (Mr), and Intrinsic Coercivity (Hc). The characterization results of Fe_3O_4/GO nanocomposites with composition variations of 40%:60%, 30%:70%, and 20%:80% were obtained using a Vibrating Sample Magnetometer (VSM).

The VSM characterization results for Fe3O4/GO composites with a 40%:60% composition ratio are presented in Figure 6 below.

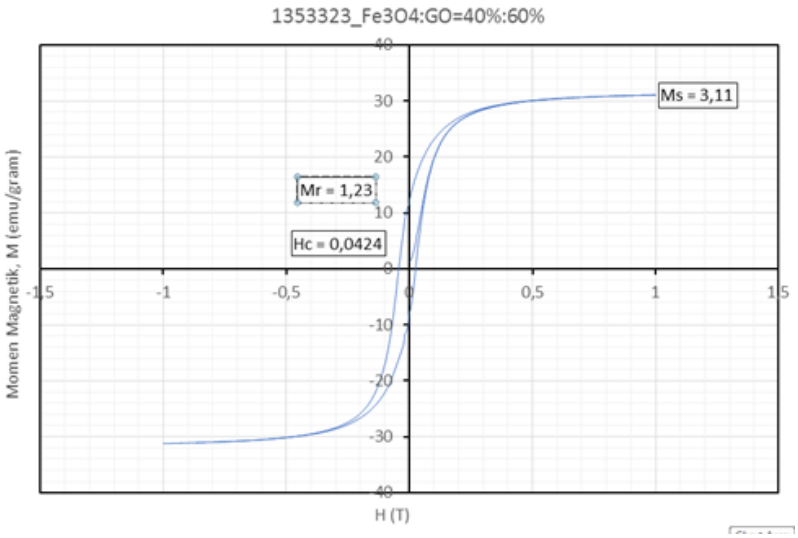

Figure 6. The hysteresis curve of Fe_3O_4/GO nanocomposite with composition variation of 40%: 60%

The VSM characterization results for Fe_3O_4/GO composites with a 30%:70% composition ratio are presented in Figure 7 below.

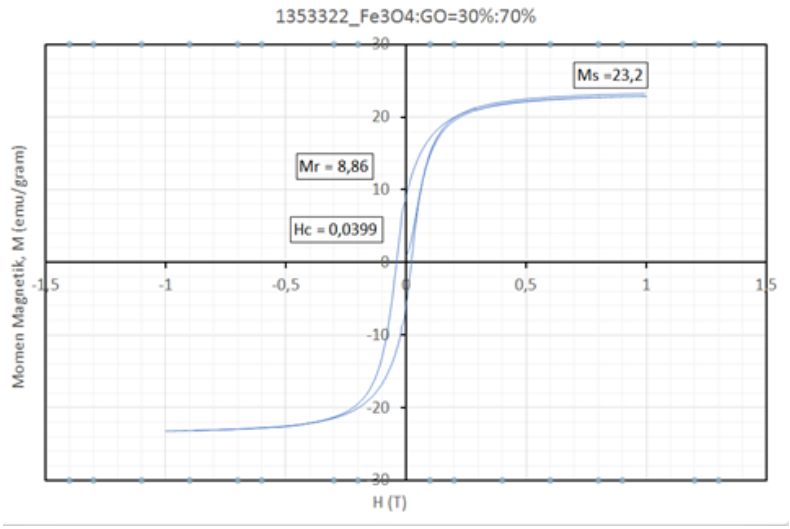

Figure 7. The hysteresis curve of Fe_3O_4/GO nanocomposite with composition variation of 30%: 70%

The VSM characterization results for Fe_3O_4/GO composites with a 20%:80% composition ratio are presented in Figure 8 below.

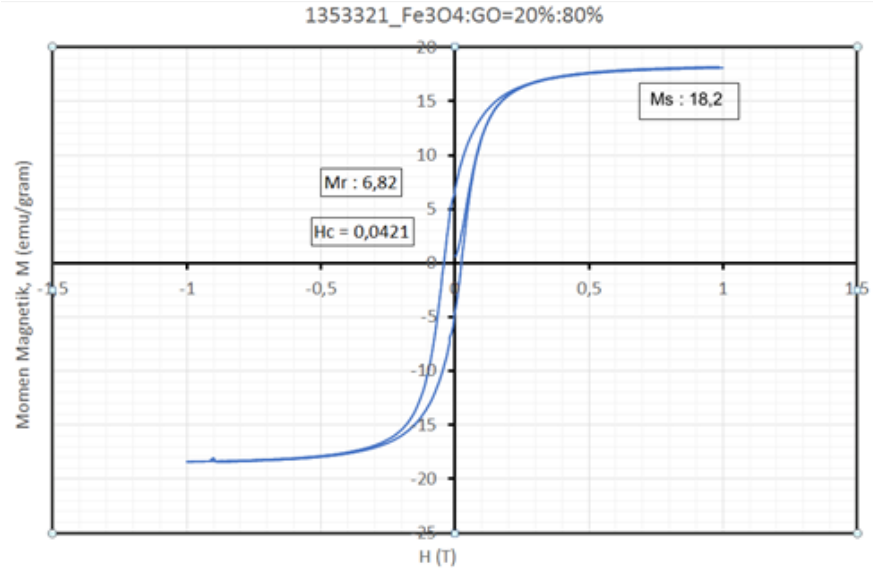

Figure 8. The hysteresis curve of Fe_3O_4/GO nanocomposite with composition variation of 20%: 80%

The magnetic properties of the Fe_3O_4/GO nanocomposite were measured using a Vibrating Sample Magnetometer (VSM) to assess the magnetic characteristics of the composite. The VSM measurement results indicated that smaller grain sizes of magnetite nanoparticles produced a stronger magnetic response. The magnetic properties of the composite are primarily influenced

by factors such as crystallite or grain size, crystallite shape and distribution, and the type of magnetic phase forming the composite structure. Intergranular exchange interactions and dipolar interactions play a significant role in determining the magnetic properties of nanocomposite magnets.

The Vibrating Sample Magnetometer (VSM) characterization results were processed using OriginPro 8.5.1 software. This software was utilized to combine the hysteresis curves for the three variations of Fe_3O_4/GO nanocomposite compositions, which are shown in Figure 9 below.

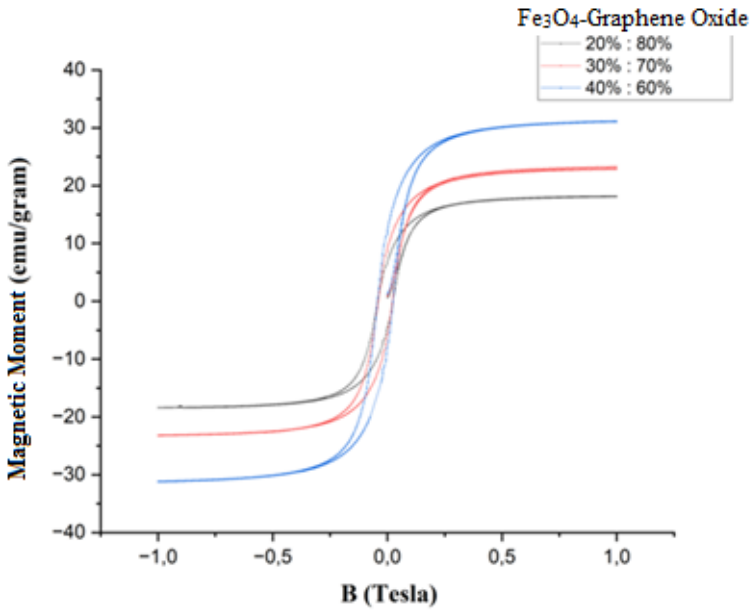

Figure 9: The hysteresis curves of Fe_3O_4/GO nanocomposites for 3 composition variations.

The values of Saturation Magnetization (Ms), Remanent Magnetization (Mr), and Intrinsic Coercivity (Hc) obtained for each sample using the Vibrating Sample Magnetometer (VSM) are presented in Table 7 below.

Table 7: The analysis results of Magentic Properties of Fe_3O_4/GO nanocomposites for 3 composition variations

Composition variations (% mass)		Intrinsic Coercivity (HC) (T)	Remanent Magnetization (Mr) (emu/gram)	Saturation Magnetization (Ms) (emu/gram)
Fe_3O_4	GO			
20 %	80 %	0,0421	6,82	18,2
30 %	70 %	0,0399	8,86	23,2
40 %	60 %	0,0424	12,3	31,1

The results in Table 7 show the properties of Fe_3O_4/GO nanocomposites with composition ratios of 40%:60%, 30%:70%, and 20%:80%. When an external magnetic field is applied, the

samples become magnetized, achieving saturation magnetization values of 31.1 emu/gram, 23.2 emu/gram, and 18.2 emu/gram. After the external magnetic field is removed, the magnetization does not drop to zero, showing remanent magnetization values of 12.3 emu/gram, 8.86 emu/gram, and 6.82 emu/gram. To reduce the magnetization to zero, an external field of 0.0424 T (424 Oe), 0.0399 T (399 Oe), and 0.0421 T (421 Oe) is required. The narrow hysteresis curve suggests that the sample is a soft magnetic material. According to previous research [31], suggests that the Fe_3O_4/GO nanocomposites with these composition variations are superparamagnetic due to their particle size, which ranges from 1 to 100 nm.

Table 5 presents the particle size results for each composition variation of Fe_3O_4/GO nanocomposites. Based on Table 7, it is observed that as the particle size increases, the coercive field also increases. This relationship applies to particles smaller than 40 nm. For smaller magnetite (Fe) nanoparticles, the barrier energy (anisotropy energy) decreases, which results in a smaller coercive field (H). As the barrier energy is reduced, a smaller external field is required to make the magnetization zero, allowing greater freedom for the magnetic moment to fluctuate. However, a deviation is seen in the sample with a 30%:70% composition variation, where the coercive field does not increase linearly with the Fe_3O_4particle size. This phenomenon was also observed in the study by Yulianti et al. [33]. It is attributed to agglomeration in the 30%:70% sample, where clumping affects the direction of the magnetic moment, restricting its freedom to fluctuate. As a result, a larger external magnetic field is needed to reduce the net magnetization to zero.

The variation in saturation magnetization values is likely due to the effect of particle size. As the particle size increases, the coercivity value also rises. Particle size plays a significant role in altering the magnetic properties of materials. Research by Yadav et al. [34] indicates that smaller particle sizes lead to lower saturation magnetization. This result supports the theory that smaller particles are more easily magnetized [35].

The VSM analysis of Fe_3O_4/GO nanocomposites showed an increase in the magnetic properties (Ms, Mr, and Hc) of GO in all composition variations, due to the incorporation of Fe_3O_4 nanoparticles. This improvement is because Fe_3O_4 nanoparticles are ferromagnetic materials, which have a structured atomic arrangement and magnetic dipole moment, allowing for a strong magnetic response when combined with GO [36]. The 40%:60% composition variation of Fe_3O_4/GO nanocomposites exhibited the best results, with the highest values for intrinsic coercivity (Hc), remanent magnetization (Mr), and saturation magnetization (Ms), which are 0.0424 T, 12.3 emu/gram, and 31.1 emu/gram.

Based on the observations above, the Fe_3O_4/GO nanocomposite can be classified as a superparamagnetic material, as it produces a magnetic response when subjected to external and remanent magnetic fields, with zero coercivity in the presence of a magnetic field. These properties make the Fe_3O_4/GO nanocomposite a promising candidate for use as a nanocarrier in drug delivery systems, particularly for cancer chemotherapy agents.

4. Conclusion

This study explores the magnetic properties of Fe_3O_4/GO nanocomposites synthesized from corn cobs waste using Vibrating Sample Magnetometer (VSM). The characterization results of Fe_3O_4/GO nanocomposites with composition variations of 40%:60%, 30%:70%, and 20%:80% were obtained using Vibrating Sample Magnetometer (VSM). VSM analysis provided data on the hysteresis curves of the Fe_3O_4/GO samples, showing variations in Saturation Magnetization (Ms), Remanent Magnetization (Mr), and Intrinsic Coercivity (Hc).

The analysis of Saturation Magnetization (Ms) and Remanent Magnetization (Mr) values revealed an increase with higher Fe_3O_4 content in GO, showing different values for the 20%:80%, 30%:70%, and 40%:60% compositions. However, a deviation in the intrinsic coercivity (Hc) value was observed, where the results were not linear due to agglomeration in the Fe_3O_4/GO nanocomposite sample, which interfered with the fluctuation of the magnetic moment. The findings suggest that the addition of Fe_3O_4 influences the magnetic properties of the nanocomposites, particularly increasing the Saturation Magnetization (Ms) and Remanent Magnetization (Mr) values, leading to a narrower hysteresis curve. Based on these characteristics, this sample classified as superparamagnetic material, it can be used as an alternative material of nanocarrier drug delivery for chemotherapeutic agents.

Acknowledgments

The author would like to express gratitude to the Head and Laboratory analysts of LLDIKTI Region X Padang, as well as the Physics and Chemistry Laboratories at Padang State University, for granting permission to conduct the research in their facilities until its completion. The fieldwork for this project was supported by the National Research and Innovation Agency of Indonesia.

References

[1] Suddarth, Brunner. "Keperawatan Medikal Bedah." Jakarta: EGC (2014).
[2] World Health Organization. Cancer. Retrieved September 16, 2023, from https://www.who.int/health-topics/cancer#tab=tab_ (2018).
[3] Riskesdas, Kemenkes. "Hasil utama riset kesehatan dasar (RISKESDAS)." Journal of Physics A: Mathematical and Theoretical 44.8 (2018): 1-200.
[4] Kemenkes, R. I. "Situasi penyakit kanker." Pusat Result dan Informasi Kesehatan (2015).
[5] Hsiao, Meng-Hsuan, et al. "Hexanoyl-chitosan-PEG copolymer coated iron oxide nanoparticles for hydrophobic drug delivery." ACS macro letters 4.4 (2015): 403-407.ss
[6] Winarti, L. (2015). Sistem penghantaran obat tertarget, macam, jenis-jenis sistem penghantaran, dan aplikasinya. STOMATOGNATIC-Jurnal Kedokteran Gigi, 10(2), 75-81.
[7] Arofik, Handika Nur, and Bayyinatul Muchtaromah. "Aplikasi Teknologi Nanopartikel Pada Pengobatan Kanker." ULIL ALBAB: Jurnal Ilmiah Multidisiplin 2.4 (2023): 1578-1585. “PDCA 12-70 data sheet,” Opto Speed SA, Mezzovico, Switzerland.

[8] Fong, Yi Teng, Chih-Hao Chen, and Jyh-Ping Chen. "Intratumoral delivery of doxorubicin on folate- conjugated graphene oxide by in-situ forming thermo-sensitive hydrogel for breast cancer therapy." Nanomaterials 7.11 (2017): 388.

[9] Hanh, Nguyen Thi, Nguyen Thi Xuyen, and Tran Thi Thanh Thuy. "Synthesis and characterization of Fe_3O_4/GO nanocomposite for drug carrier." Vietnam Journal of Chemistry 56.5 (2018): 642-646.

[10] Song, Meng-Meng, et al. "Lactoferrin modified graphene oxide iron oxide nanocomposite for glioma-targeted drug delivery." Materials Science and Engineering: C 77 (2017): 904-911.

[11] Meilianti, Meilianti. "Pembuatan Karbon Aktif dari Arang Tongkol Jagung Dengan Variasi Konsentrasi Aktivator Natrium Karbonat (Na_2CO_3)." Jurnal Distilasi 5.1 (2020): 14-20.

[12] Bete, Yuditha Ignasia, et al. "Kajian Awal Sifat Optik Graphene Oxide Berbahan Dasar Arang Tongkol Jagung Yang Disintesis Dengan Metode Liquid Phase Exfoliation (Lpe)." Jurnal Fisika: Fisika Sains Dan Aplikasinya 4.2 (2019): 114-120.

[13] Nurzam, Fildzah Rudyah Putri. "Pengaruh komposisi $CoFe_2O_4$terhadap sifat listrik nanokomposit $CoFe_2O_4$/pani yang disintesis dengan metoda sol-gel ($CoFe_2O_4$composition influence on the electrical properties of the $CoFe_2O_4$/PANI nanocomposite synthesized by the sol-gel method)." PILLAR OF PHYSICS 12.1 (2019).

[14] W. S. B. Dwandaru, "Nanomaterial Graphene Oxide Sintesis Dan Karakterisasinya," pp. 1–156, (2019).

[15] Jaleh, Babak, et al. "Synthesis, characterization, magnetic and catalytic properties of GO/Fe_3O_4." Journal of Materials Science: Materials in Electronics 28 (2017): 4974-4983.

[16] Gosai, Agnivo, et al. "Application of functionalized graphene oxide based biosensors for health monitoring: Simple graphene derivatives to 3D printed platforms." Biosensors 11.10 (2021): 384.

[17] Jiříčková, Adéla, et al. "Synthesis and applications of graphene oxide." Materials 15.3 (2022): 920.

[18] Alam, Syed Nasimul, Nidhi Sharma, and Lailesh Kumar. "Synthesis of graphene oxide (GO) by modified hummers method and its thermal reduction to obtain reduced graphene oxide (rGO)." Graphene 6.1 (2017): 1-18.

[19] R. Nanda, "Analisis Struktur Mikro Oksida Graphene Dari Limbah Tempurung Kelapa Tua," PILLAR Phys., vol. 15, no. 1, pp. 69–76, 2022.

[20] M. Ikhsan and R. Ramli, "Measurements and analysis of crystal structures of activated carbon of empty fruit bunch from oil palm biomass waste," in Journal of Physics: Conference Series, IOP Publishing, 2020, p. 12031.

[21] J. Wang, E. C. Salihi, and L. Šiller, "Green Reduction Of Graphene Oxide Using Alanine," Mater. Sci. Eng. C, vol. 72, pp. 1–6, 2017.

[22] M. Hapsari, A. H. Cahyana, S. H. Oktavia, and A. R. Liandi, "Synthesis Of Spirooxindole-Pyrrolizidine Compounds Using Fe_3O_4/GO Catalyst And Their Bioactivity Assays," Rasayan J. Chem, vol. 13, no. 4, pp. 2317–2324, 2020.

[23] M. B. P. Honorisal, N. Huda, T. Partuti, and A. Sholehah, "Sintesis Dan Karakterisasi Grafena Oksida Dari Tempurung Kelapa Dengan Metode Sonikasi Dan Hidrotermal," J. Sains dan Teknol., vol. 16, no. 1, pp. 1–11, 2020.

[24] N. Syakir, R. Nurlina, S. Anam, A. Aprilia, and S. Hidayat, "Kajian Pembuatan Oksida Grafit Untuk Produksi Oksida Grafena Dalam Jumlah Besar," J. Fis. Indones., vol. 19, no. 56, pp. 26–29, 2015.

[25] F. Contreras, Jesus & Briones, "Graphene Oxide Powders With Different Oxidation Degree, Prepared By Synthesis Variations Of The Hummers Method," Mater. Chem. Phys., vol. 153, pp. 209–220, 2015.

[26] Purwaningsih, Hariyati, Widiyastuti Widiyastuti, and Heru Setyawan. "Synthesis and characterization of magnetite/graphene nanocomposite material for electrocatalyst of zinc-air battery chatode." AIP Conference Proceedings. Vol. 2384. No. 1. AIP Publishing, 2021.

[27] Rukman, N. K., et al. "GO-Fe_3O_4 Nanocomposite from coconut shell: synthesis and characterization." IOP Conference Series: Earth and Environmental Science. Vol. 217. No. 1. IOP Publishing, 2019.

[28] Putra, Gilang, et al. "Synthesis of green Fe3+/glucose/rGO electrode for supercapacitor application assisted by chemical exfoliation process from burning coconut shell." AIP Conference Proceedings. Vol. 1945. No. 1. AIP Publishing, 2018.

[29] A. Hardiansyah, E. R. Chaldun, and A. F. Idzni, "Magnetic Reduced Graphene Oxide As Advanced Materials For Adsorption Of Metal Ions," J. Sains Mater. Indones., vol. 18, no. 4, pp. 185–189, 2018.

[30] L. P. Lingamdinne, J. R. Koduru, and R. R. Karri, "A Comprehensive Review Of Applications Of Magnetic Graphene Oxide Based Nanocomposites For Sustainable Water Purification," J. Environ. Manage., vol. 231, pp. 622–634, 2019.

[31] Dewanto, A. S., et al. "Composites of Fe_3O_4 /SiO2 from natural material synthesized by co-precipitation method." IOP Conference Series: Materials Science and Engineering. Vol. 202. No. 1. IOP Publishing, 2017.

[32] Barbeta, Vagner Bernal, et al. "Magnetic properties of Fe_3O_4 nanoparticles coated with oleic and dodecanoic acids." Journal of Applied Physics 107.7 (2020).

[33] Yulianti, Sovia, and Yenni Darvina. "Pengaruh komposisi $CoFe_2O_4$ terhadap sifat magnetik nanokomposit $CoFe_2O_4$/PVDF yang disintesis dengan metode sol gel (The effect of $CoFe_2O_4$ composition on the magnetic properties of the $CoFe_2O_4$/PVDF nanocomposites synthesized by the sol gel method)." Pillar of Physics 13.1 (2020).

[34] Yadav, Raghvendra Singh, et al. "Superparamagnetic ZnFe2O4 nanoparticles-reduced graphene oxide-polyurethane resin based nanocomposites for electromagnetic interference shielding application." Nanomaterials 11.5 (2021): 1112.

[35] Kiswanto, Heri, et al. "Struktur Kristal dan Sifat Kemagnetan Nanopartikel Mn-Ferrite yang Disintesis dari Bahan Alam Pasir Besi." Jurnal Fisika Unand 10.4 (2021): 413-420.

[36] Marta, Romizah, and Yenni Darvina. "Pengaruh komposisi $MnFe_2O_4$ terhadap sifat magnetik nanokomposit $MnFe_2O_4$/PVDF yang di preparasi dengan metode spin coating (The effect of the $MnFe_2O_4$ composition on the magnetic properties of the $MnFe_2O_4$/PVDF nanocomposites prepared by the spin coating method)." PILLAR OF PHYSICS 13.1 (2020).